# Connexin hemichannels as candidate targets for cardioprotective and anti-arrhythmic treatments

Luc Leybaert,[1] Maarten A.J. De Smet,[1] Alessio Lissoni,[1] Rosalie Allewaert,[1] H. Llewelyn Roderick,[2] Geert Bultynck,[3] Mario Delmar,[4] Karin R. Sipido,[2] and Katja Witschas[1]

[1]Physiology Group, Department of Basic and Applied Medical Sciences, Ghent University, Ghent, Belgium. [2]Laboratory of Experimental Cardiology, Department of Cardiovascular Sciences, and [3]Laboratory of Molecular and Cellular Signaling, Department of Cellular and Molecular Medicine, KU Leuven, Leuven, Belgium. [4]Leon H. Charney Division of Cardiology, School of Medicine, New York University, New York, USA.

**Connexins are crucial cardiac proteins that form hemichannels and gap junctions. Gap junctions are responsible for the propagation of electrical and chemical signals between myocardial cells and cells of the specialized conduction system in order to synchronize the cardiac cycle and steer cardiac pump function. Gap junctions are normally open, while hemichannels are closed, but pathological circumstances may close gap junctions and open hemichannels, thereby perturbing cardiac function and homeostasis. Current evidence demonstrates an emerging role of hemichannels in myocardial ischemia and arrhythmia, and tools are now available to selectively inhibit hemichannels without inhibiting gap junctions as well as to stimulate hemichannel incorporation into gap junctions. We review available experimental evidence for hemichannel contributions to cellular pro-arrhythmic events in ventricular and atrial cardiomyocytes, and link these to insights at the level of molecular control of connexin-43–based hemichannel opening. We conclude that a double-edged approach of both preventing hemichannel opening and preserving gap junctional function will be key for further research and development of new connexin-based experimental approaches for treating heart disease.**

## Introduction

The coordinated functioning of the heart as a pump heavily relies on communication between more than 3 billion cardiomyocytes via connexin-based gap junctions (GJs). GJs connecting cardiomyocytes and cells in conduction tissues distribute electrical impulses over this cellular syncytial network, acting to steer and synchronize the contraction-relaxation sequence of atria and ventricles during each pump cycle. GJs are a special kind of channel, as they are composed of two hemichannels (HCs) originating from distinct juxtaposed cells sharing the junctional channel. Like their HC counterparts, GJs pass ions, metabolites, and signaling molecules with a molecular weight (MW) below about 1.5 kDa, e.g., $Na^+$, $K^+$, $Ca^{2+}$, ATP, cAMP, inositol 1,4,5-trisphosphate, and many others (1–3).

The importance of GJs becomes clear from the huge turnover rate of its connexin building blocks, characterized by a half-life of approximately 1–5 hours for the 43-kDa connexin-43 (Cx43), a major connexin in the heart (4, 5). Such a high turnover rate allows continuous remodeling of GJs to adapt to varying degrees of cardiac pump load. This is associated with a continuous Cx43 stream through the endoplasmic reticulum/Golgi network, where Cx43 oligomerizes (6), followed by its arrival in the plasma membrane assembled as hexameric HCs. From there, HCs migrate laterally in the sarcolemmal lipid bilayer toward a zone called the perinexus where they coalesce with the edges of existing GJs, known as the nexus zone (4, 7). HCs subsequently dock head to head with their counterparts on neighboring cells, forming GJ channels that combine into channel arrays organized as junctional plaques. The connexin's life as a GJ ends with plaque-associated GJs being internalized as "annular GJs" or connexosomes, which are further degraded via endolysosomal or autophagosomal pathways (refs. 4, 8–11; and reviewed in ref. 12).

The high Cx43 turnover rate also implies a continuous process of HC delivery to the sarcolemma. Before their incorporation into GJs, HCs are closed to prevent membrane leakage of intracellular and extracellular factors through these highly conductive channels (~220 pS electrical conductivity per Cx43 HC; compare with ~5 pS for L-type $Ca^{2+}$ channels). While open GJs close under certain conditions, such as ischemia, HCs react oppositely and open under ischemic or inflammatory conditions (13–16). The functional consequences of HC opening have been difficult to investigate under ex vivo or in vivo conditions, mainly because connexin channel inhibitors used for this purpose affect both GJs and HCs. Since the finding that certain Cx43 mutants distinctly affect HC versus GJ function (17, 18) and the introduction of peptides such as Gap19 that inhibit Cx43 HCs without inhibiting GJs (19), more detailed and conclusive studies have been possible. Here, we discuss how inhibition of HCs can be used to protect against experimental ischemic cardiac injury and review recent experimental evidence on their possible contribution to arrhythmogenic processes. Considerations on mitochondrial Cx43 HCs are not covered here, as these have been recently reviewed elsewhere (20).

**Conflict of interest:** MD received research support from Rocket Pharmaceuticals Inc. (New York, New York, USA) in the fiscal year preceding the date of original submission. LL, MAJDS, and AL are inventors on European Patent EP3835316A1 related to molecules for treating or preventing cardiac diseases.

**Reference information:** *J Clin Invest*. 2023;133(6):e168117.
https://doi.org/10.1172/JCI168117.

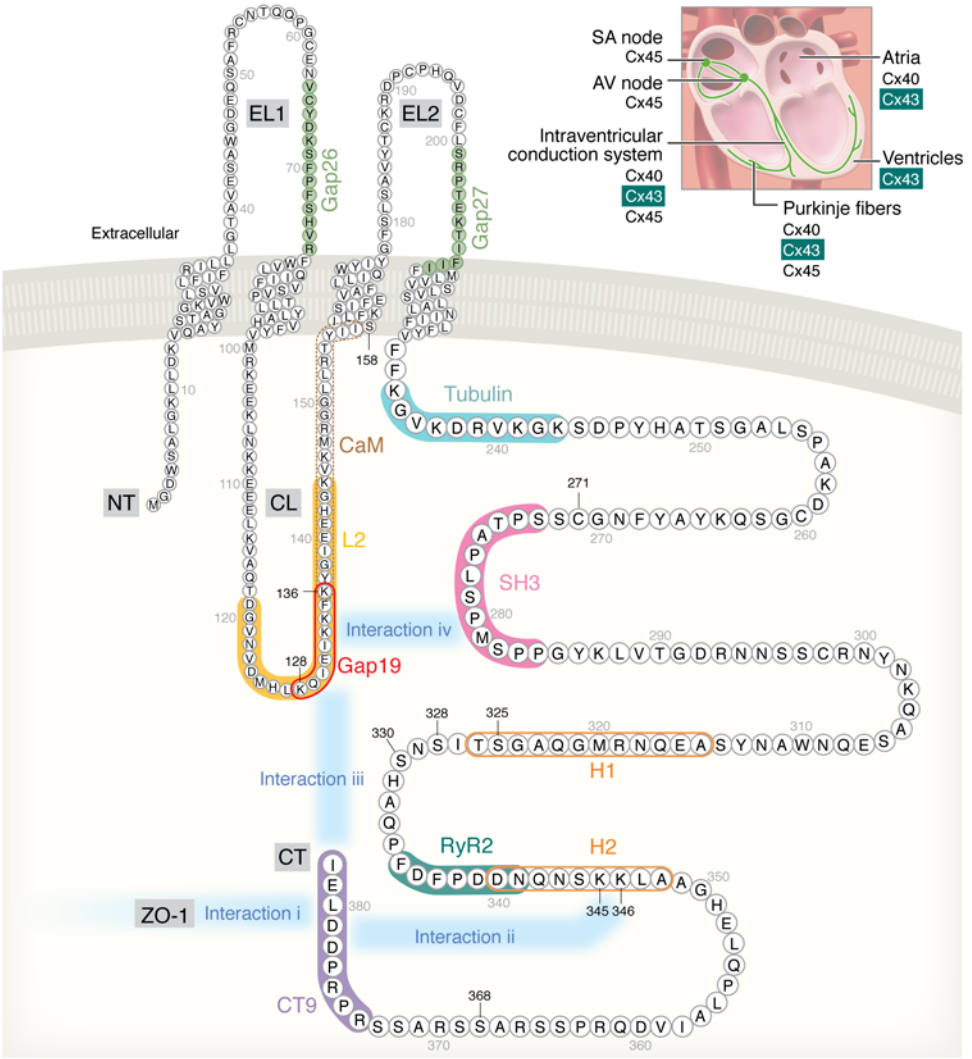


**Figure 1. Connexins in the heart and Cx43 topology with indication of crucial sites and interactions that are discussed in this Review.** The upper right image illustrates expression of Cx40, Cx43, and Cx45 in heart muscle, conduction tissues, and nodes. Cx43 is present in most of the tissues, except for the sinoatrial and atrioventricular nodes. Cx40 prevails in atrial cardiomyocytes and in the His-Purkinje system (23, 25, 152, 153), while Cx45 is primarily expressed in the conduction system (23). The Cx43 topology scheme indicates various regions and sequences that are discussed in this Review. Gap19, L2, Gap26, Gap27, and CT9 are sequences that have been used as mimetic peptides affecting Cx43 channel function as well as Cx43 interaction within or outside the protein. The sequences marked "Tubulin" and "RyR2" (ryanodine receptor-2) indicate interaction sites with these respective proteins. "CaM" indicates a calmodulin interaction site. "SH3" denotes an Src homology binding domain. H1 (315 to 326) and H2 (340 to 348) are α-helical structures. Ser325, Ser328, Ser330, and Ser368 are phosphorylation sites, while Cys271 is a nitrosylation site, which are discussed in the main text. NT, N-terminal end; CT, C-terminal end; EL1 and EL2, extracellular loops 1 and 2; CL, cytoplasmic loop; ZO-1, zonula occludens 1.

For background information on the role of GJ channels and HCs in cardiac ischemia and arrhythmia, we refer the reader to comprehensive reviews in refs. 12, 21, and 22.

## Preserving GJs and inhibiting HCs in cardiac disease

Cardiomyocytes and cells of the conduction system in the normal human adult heart mainly express Cx40, Cx43, and Cx45 (23–25). Cx43, a ubiquitously expressed connexin encoded by the *GJA1* gene, is the main connexin in ventricular cardiomyocytes, and in the His-Purkinje system, which facilitates rapid electrical conduction in heart ventricles (23–25) (Figure 1).

The roles of GJs formed by atrial Cx40/Cx43 and ventricular Cx43 have been extensively investigated in cellular and animal models of cardiac ischemia/reperfusion (12, 26). GJs close under ischemic conditions as a consequence of cytosolic modulation by intracellular acidification, increased cytoplasmic $Ca^{2+}$ concentration ($[Ca^{2+}]_i$), and connexin dephosphorylation (27–29), thereby hampering impulse conduction over the specialized conduction tissues and myocardial tissue. However, cardiac impulse conduction is characterized by a large degree of "coupling reserve," meaning that Cx43 protein levels must dip below approximately 20% before impulse conduction velocity decreases or the QRS interval, which partially reflects the fast upstroke action potential (AP) depolarization phase, becomes prolonged (30–33). Impulse conduction involves two components: voltage-gated $Na^+$ channels propagating the depolarization wave over the sarcolemma and GJs passing the signal to neighboring cells (34). Moreover, Cx43 protein levels affect sarcolemmal $Na^+$ channel expression at the intercalated disk (ID) (35), which introduces some nonlinearity in the relationship between Cx43 expression and impulse conduction. Moreover, coupling by so-called "ephaptic" mechanisms is also thought to contribute, entailing extracellular charge accumulation at the ID that is capacitively coupled to the adjacent cell interior, pushing it above threshold to promote AP propagation (reviewed in refs. 36, 37). Given the substantial coupling reserve and the many factors that influence cardiac AP propagation, it was somewhat surprising that enhancement of GJ coupling by preservation of Cx43 phosphorylation with ZP123 peptide, or its non-peptide version Gap134 (also known as danegaptide), limited infarct size, maintained conduction velocity, and prevented ventricular fibrillation in acute coronary ischemia studied in various animal models

**Table 1. Protective effect of Cx43-based peptides on ischemic injury in heart and brain**

| Experimental model | Peptide | Model details and treatment | Effect | Ref. |
|---|---|---|---|---|
| Cardiac I/R, mouse | Gap19 | 30/120 min LAD ligation/reperfusion; 25 mg/kg Gap19 i.v. 10 min before ligation | Infarct size ~1/5 reduced | 19 |
| Cardiac I/R, rat | Gap19 | 30/120 min I/R in Langendorff-perfused hearts; 0.05 μM Gap19 before ischemia and before reperfusion | Infarct size ~1/4 reduced | 54 |
| Brain stroke, mouse | TAT-Gap19 | MCAO without reperfusion; 7.5 μmol/kg TAT-Gap19 i.p. 2 h after occlusion | Infarct size ~3/4 reduced 4 d after stroke induction | 55 |
| Cardiac I/R, mouse | αCT1 | 30/40 min I/R in Langendorff-perfused hearts; 10–50 μM αCT1 | LV contractile function ~4-fold improved | 56 |
| Cardiac I/R, mouse | αCT11 (CT9) | 30/40 min I/R in Langendorff-perfused hearts; 10–50 μM αCT11 | LV contractile function >5-fold improved | 56 |

I/R, ischemia/reperfusion; LAD, left anterior descending coronary artery; MCAO, mid-cerebral artery occlusion; LV, left ventricle.

(38–44). Unfortunately, no such benefit was observed in a human clinical study in which effects of danegaptide on infarct size or left ventricular ejection fraction were examined in myocardial infarction patients 3 months after thrombolysis treatment (45). Several reasons may underlie the lack of effect, including variability in patient pathology, incomplete mechanistic understanding of GJ enhancers, and the risky business of focusing on GJs as a single target. In fact, the effect of GJ enhancers in animal models of brain disease, which aim to preserve astrocytic syncytial connectivity, is also variable, as they reduce infarct size in stroke but enhance seizure activity in epilepsy (refs. 46, 47; and reviewed in ref. 48).

Around the turn of the century, evidence became available demonstrating HC opening in cardiomyocytes exposed to metabolic inhibition or ischemia/reperfusion (13, 14, 49), and showing protective effects of HC inhibition with Gap26 or Gap27 peptides against ischemic injury in isolated Langendorff-perfused rat hearts (50–52). Gap26/27 peptides, mimicking sequences on the extracellular loops of Cx43 (Figure 1), rapidly inhibit HCs and, with some delay, also inhibit GJs (ref. 53; and reviewed in ref. 22). The latter effect is obviously not acceptable for realistic treatment purposes. Further work with the more selective Cx43 HC peptide inhibitor Gap19, a nonapeptide sequence in the cytoplasmic loop (CL) (Figure 1), demonstrated protection of ventricular cardiomyocytes against metabolic inhibition–induced volume overload and cell death (19). Gap19 treatment also protected against cardiac ischemia/reperfusion injury in mice, reducing the infarct size by approximately one-fifth (19) (Table 1). Recent work with Gap19 in Langendorff-perfused rat hearts demonstrated approximately one-fourth infarct size reduction (54). For comparison, in a mouse permanent stroke model, treatment with TAT-Gap19 (containing the HIV-TAT cell-permeation sequence), aiming to target astrocytic Cx43 HCs, gave an approximately three-fourths reduction in brain infarct (55). It remains to be determined whether TAT-Gap19, which has a 5-fold better membrane permeability compared with Gap19 (19), could enhance its protective potential against cardiac ischemia/reperfusion injury.

αCT1 is another Cx43-based peptide that protects against ischemia/reperfusion injury in Langendorff-perfused mouse hearts (56). It is composed of the last 9 amino acids of the C-terminal (CT) end of Cx43 (Figure 1, CT9) coupled to an antennapedia cell-permeation sequence. Pre-ischemic administration of αCT1 demonstrated a strong improvement of left ventricular contractile function, and protection was even larger with CT9 peptide without antennapedia sequence, dubbed αCT11 (56) (Table 1). As CT9/αCT11 is not membrane permeable, it was hypothesized that the peptide entered the cells through open HCs.

Mechanistically, αCT1 prevented Cx43 remodeling known as "Cx43 lateralization," i.e., increased Cx43 presence at lateral sides close to the ID, in a left ventricular cryoinjury model (57). It also reduced inducible arrhythmias and increased ventricular depolarization rate. The αCT1/αCT11 peptides are proposed to interfere with the interaction of the Cx43 CT (last 4 amino acids: DLEI sequence) with the PDZ2 binding domain of the zonula occludens scaffolding protein ZO-1 (58–60) (Figure 1, interaction 1). Consequently, Cx43 HCs lose their association with ZO-1, dock with their counterparts on the opposed membrane, and integrate as GJ channels at the edge of GJ plaques, a process that decreases HC presence in the perinexus and thus reduces Cx43 lateralization.

Besides interaction of the Cx43 CT end with the PDZ2 binding domain, the CT9 region of Cx43 also engages in molecular interactions with the CT-located α-helical H2 region (Figure 1, interaction 2). The αCT1/αCT11 peptides also interfere with this CT9-H2 interaction, thereby enhancing PKCε phosphorylation of Ser368 (Figure 1), which is crucial for their protective effects (56, 57). Phosphorylation of Ser368 is known to restrain the passage of high-MW substances through HCs (61–63), which may contribute to the protective potential of αCT1/αCT11. At the level of GJs, Ser368 phosphorylation enhances cell-cell coupling in response to ZP123 peptide (64), but decreased coupling has also been reported (65, 66).

## Molecular interactions controlling Cx43 channel function

Connexins located in the perinexus and nexus interact with multiple partners, including cytoskeletal molecules, mechanical junctions, and ion channel complexes (67), which affect their transport and organizational stability as well as channel functions. Most of these interactions, some of which have already been touched upon, involve the CT tail of Cx43 that forms a true hub, affecting not only connexin channel transport and function but also the activity of the interacting partner proteins. Below, we briefly highlight some of these interactions for their involvement in opposite effects on GJs versus HCs and their importance in HC-linked arrhythmogenic signaling.

*Cx43 tail-loop interactions govern HC opening.* In addition to the interactions discussed above, the Cx43 CT tail also interacts with the CL-located L2/Gap19 region (Figure 1, interaction 3). In particular, interaction of the CT9 region with the L2/Gap19 region is necessary to bring Cx43 HCs to the "available to

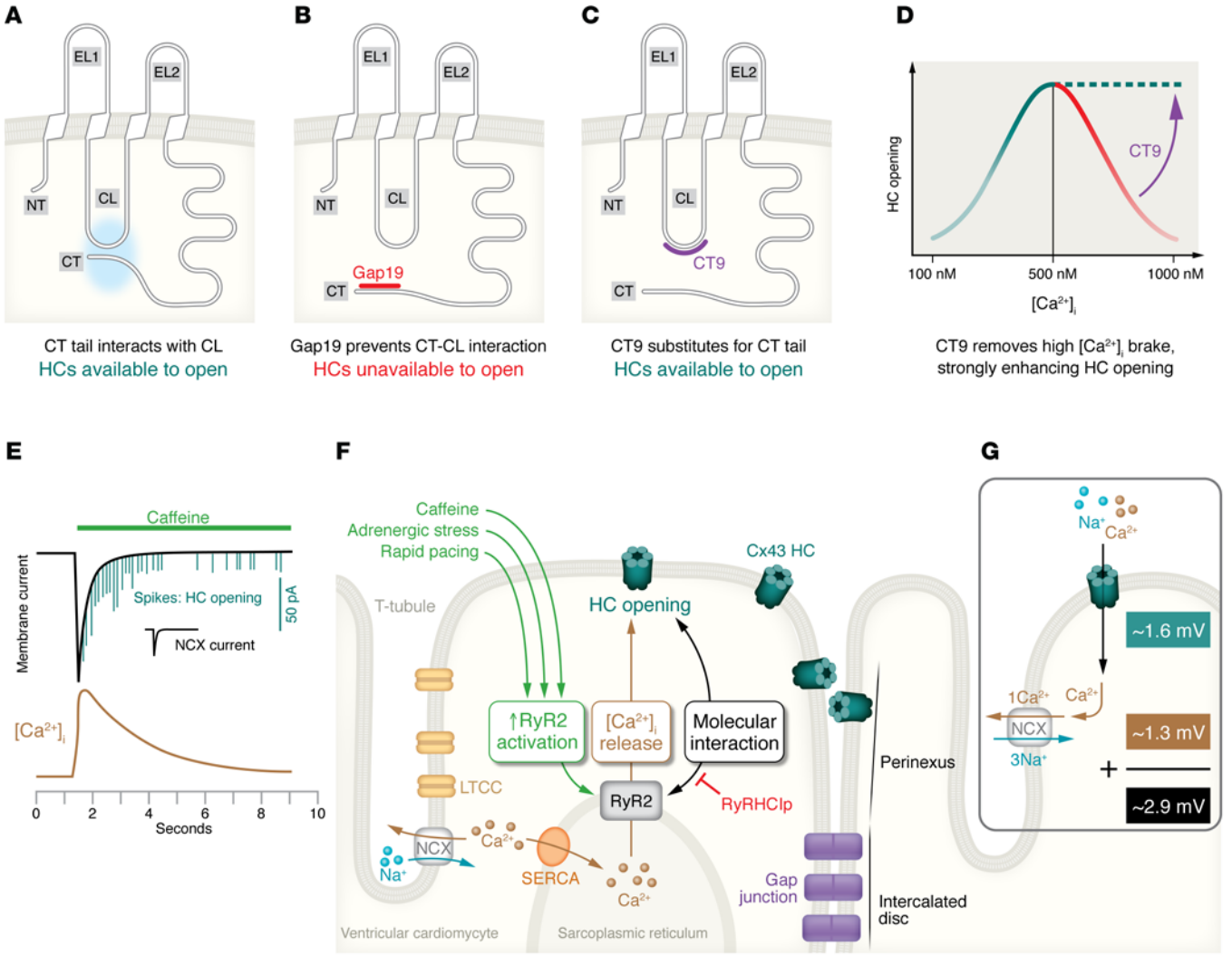


**Figure 2. Cx43 HC activation in ventricular cardiomyocytes.** (**A**–**C**) Cx43 HC states and the effect of Gap19 and CT9 peptides. (**A**) Interaction of the CT tail with the CL brings HCs into the "available to open" state. (**B**) Gap19 interaction with the CT prevents CT-CL interaction, making HCs unavailable for opening. (**C**) CT9 peptide interaction with the CL brings HCs into the "available to open" state. (**D**) Bell-shaped $[Ca^{2+}]_i$ dependency of HC opening. CT9 removes HC inhibition at above 500 nM $[Ca^{2+}]_i$ (dashed line), thereby strongly enhancing HC opening. (**E**) Caffeine activation of RyRs triggers $[Ca^{2+}]_i$ elevation (brown trace) followed by NCX current (black) associated with $Ca^{2+}$ extrusion. Spiking HC opening activity appears superimposed on the NCX current. At the start of caffeine application, simultaneous (stacked spikes) HC openings can be distinguished resulting from up to three HCs. (**F**) HC opening in ventricular cardiomyocytes requires three conditions: (a) activation of RyR2 by caffeine, adrenergic stress, or rapid electrical pacing; (b) $[Ca^{2+}]_i$ elevation; and (c) molecular interaction between RyR2 and Cx43 HCs (inhibited by RyRHClp peptide). (**G**) Open HCs carry inward current producing about 1.6 mV depolarization per HC (at –70 mV diastolic potential). HC $Ca^{2+}$ entry triggers microdomain $Ca^{2+}$ elevation that is extruded by NCX activity, adding another 1.3 mV depolarization, yielding almost 3 mV depolarization per HC. HC opening events are brief (~8 milliseconds on average) but sufficiently long to obtain steady-state membrane charge redistribution and achieve the approximately 3 mV depolarization estimate.

open" state (68, 69) (Figure 2A), from which HC opening can be triggered by electrical stimulation or elevation of the cytoplasmic $Ca^{2+}$ concentration ($[Ca^{2+}]_i$). The $[Ca^{2+}]_i$-dependency of HC opening in ventricular cardiomyocytes is characterized by a bell-shaped relation (70) (Figure 2D) whereby Cx43 HCs open in the 100- to 500-nM $[Ca^{2+}]_i$ range but close again upon further $[Ca^{2+}]_i$ elevation to 500–1,000 nM. HC opening involves $Ca^{2+}$/calmodulin (CaM) signaling and interaction with a CL-located CaM binding region (71, 72) (Figure 1). The loss of the response above 500 nM relates to CT linkage to the actomyosin cytoskeleton that disrupts CT-CL interaction (reviewed in refs. 73, 74). The bell-shaped $[Ca^{2+}]_i$-dependency of Cx43 HC opening is also observed in Cx43-expressing noncardiac cells (71, 75, 76). An important difference is that ventricular cardiomyocytes require two factors to trigger HC opening at negative diastolic membrane potential: a $[Ca^{2+}]_i$ elevation combined with simultaneous activation of the ryanodine receptor (RyR) by, e.g., caffeine or 4-chloro-*m*-cresol (70, 77). Note that these requirements are not necessary for electrical activation of Cx43 HC opening triggered by stepping of the membrane potential ($V_m$) to positive voltages (70, 75).

In addition to the CT9 tail interaction with the CL-located L2/Gap19 region, a second CT-located SH3-binding domain (Figure

**Table 2. Pharmacological properties of Gap19/TAT-Gap19**

| Peptide | Property/parameter | Value |
|---|---|---|
| Gap19 | $K_D$ for interaction with Cx43 CT tail | ~2.5 μM |
| Gap19 | $IC_{50}$ for HC inhibition; intracellular application | ~6.5 μM |
| Gap19 | Hill slope for HC inhibition; intracellular application | −2 |
| Gap19 | $IC_{50}$ for HC inhibition; extracellular application | ~47 μM |
| TAT-Gap19 | $IC_{50}$ for HC inhibition; extracellular application | ~7 μM |

Data based on ref. 19.

1, interaction 4) is also able to interact with the L2/Gap19 region and switch HCs to the "available to open" state (69).

Lowering of extracellular $Ca^{2+}$ below approximately 0.5 mM is also a well-established trigger for HC opening, which occurs as a result of diminished $Ca^{2+}$ interactions with negatively charged residues at the outer pore side of the HC (78). In principle, HC opening triggered by low extracellular $Ca^{2+}$ should be independent of CT-CL interactions. However, low extracellular $Ca^{2+}$ conditions may activate $[Ca^{2+}]_i$ dynamics, thereby recruiting tail-loop–dependent HC opening from the intracellular side (79).

*L2 and Gap19 prevent Cx43 tail-loop interactions*. Investigations on CT-CL control of Cx43 HC opening led to the identification of the Cx43 HC peptide inhibitors L2 and Gap19 (reviewed in refs. 22, 80) (Figure 1). L2 peptide was initially developed with the aim of preventing GJ closure upon intracellular acidification (see next paragraph) but was further scrutinized and found to act as a Cx43 HC inhibitor in various Cx43-expressing cells (68). Gap19 (19) is located within the L2 region, with residues 130–136 being part of a sequence that is crucial for interaction with the CT (81–84). Its CT binding was found to be stronger than that of L2 peptide, and it demonstrated pharmacological properties shown in Table 2. Gap19 brings Cx43 HCs into the "unavailable to open" state (Figure 2B). The peptide does not inhibit GJs upon brief exposure (hours) but enhances GJ coupling upon 24- to 48-hour incubation (~50% increase after 48 hours) (19). Gap19 is not a pore blocker but a gating modifier that reduces open-state gating (~220 pS) while increasing substate gating (~80 pS) (85), restricting the permeation to low-MW substances.

*L2 peptide prevents GJ closure*. L2 peptide was initially developed with the aim of preventing closure of Cx43-based GJs upon intracellular acidification, as occurs in cardiac ischemia (86, 87). The finding that L2 prevents GJ closure as well as HC opening has stimulated the search for other peptides fulfilling this specific purpose (88). For example, the octapeptide RRNYRRNY prevents GJ closure and inhibits plasmalemmal as well as mitochondrial HC opening (89). The insight that HC assembly into a GJ channel completely alters the functional outcome of tail-loop interactions has led to the understanding that the two channel types are distinctly regulated, often in opposite ways. As such, interfering with CT-CL interaction has the dual potential of preventing both the closure of Cx43 GJs and the opening of HCs, which offers an interesting opportunity to follow up on the disappointing outcome of the danegaptide study on myocardial infarction patients (45) with new candidate molecules based on RRNYRRNY and CyRP-71 "RXP"-type Cx43-binding peptides (88).

*CT9 enhances HC function and stimulates GJ incorporation of HCs*. In contrast to Gap19/L2, CT9 peptide enhances Cx43 HC function (19, 68, 90), and increases spiking HC opening activity in ventricular cardiomyocytes from mice (Figure 2, C and D) and pigs (77). The increased HC function results from two effects: first, CT9 peptide substitutes for the endogenous CT9 sequence, thereby maintaining HCs in the "available to open" state (Figure 2C). Second, CT9 peptide removes HC inhibition at above 500 nM $[Ca^{2+}]_i$, thereby strongly enhancing HC opening activity (68, 76) (Figure 2D).

Additionally, as delineated in the previous section, CT9 peptide (αCT1/αCT11) competes with the endogenous CT sequence for access to PDZ2/ZO-1, thereby stimulating HC incorporation into GJ plaques and reducing the lateralized HC pool and its associated channel opening activity. Increased channel gating obviously occurs faster than the process of HC incorporation into GJs, separating these two distinct effects along the timeline, resulting in acutely enhanced HC function followed by a slower phase of HC recruitment toward GJs associated with decreased HC activity and improved GJ coupling.

*Combining HC inhibition with stimulation of HC incorporation into GJs*. Can inhibition of HC opening and prevention of GJ closure be combined with enhancement of HC incorporation into GJs? In principle, combined treatment with Gap19 and CT9-based αCT1/αCT11 (to inhibit HC function as well as reduce HC presence in lateral membranes) looks like an interesting option for further exploration. However, in vivo data in mice demonstrated that such coadministration results in the mutual canceling of each peptide's effect (91), either as a consequence of direct Gap19-CT9 interaction before they reach their respective targets on the Cx43 protein (68), or by the balancing of their functional effects on HCs. Alternatively, sequential administration of Gap19 to acutely inhibit HC opening followed by delayed intervention with CT9-based tools to enhance HC incorporation into GJs may be an option. However, such a phased approach would come with the risk of a temporary CT9-induced increase in HC activity and associated arrhythmic consequences (discussed in the next section). Further work is necessary to develop tools that stimulate HC insertion into GJs without first activating HC opening. Given the multitude of interactions of Cx43, either within a single Cx43 subunit, between subunits, or with other proteins, the field is open for further discovery.

*Tubulin and actin control HC trafficking and function*. The Cx43 CT contains a tubulin-binding motif that is responsible for direct interaction with microtubules (92, 93) (Figure 1), mediating forward delivery of Cx43-containing vesicles to the perinexus (4, 7, 94, 95) steered by the microtubule plus-end tracking protein EB1 (96). Upon arrival in the subsarcolemmal zone, Cx43 colocalizes with non-sarcomeric β-actin via intermediate accessory proteins such as ZO-1 and/or drebrin (97). Both proteins are likely candidates to function as intermediates between actin and Cx43 and may be involved in disrupting CT-CL interaction and HC closure at high $[Ca^{2+}]_i$ (Figure 2D). The Cx43 CT-tubulin interaction is prevented by phosphorylation of Tyr247 by Src/Tyk2, which is modulated in a CaM-dependent manner (98–100).

*Cx43 interacts with RyRs and controls HC opening*. A recent study using super-resolution microscopy revealed that, in mouse left ventricular cardiomyocytes, about half of the dyadic RyR2s colocalize within about 20 nm of Cx43 (77). Not only RyR2 but

also sarcolemmal $Ca_v1.2$ and $Na^+/Ca^{2+}$ exchange (NCX) transporter protein colocalized with Cx43, with 30% to 50% positioned within 20 nm distance from Cx43 (77). Importantly, these colocalization data were obtained from the cell end/peri-ID region where Cx43 is abundantly present, and not from other regions or the cell interior. These findings place Cx43 in direct proximity to the major players involved in $[Ca^{2+}]_i$ regulation and excitation-contraction coupling in the heart. The colocalization between Cx43 and RyR2 was pinned down to an interaction between a short aspartate-rich sequence on the CT tail that includes part of the α-helical H2 region on the Cx43 CT tail (70) (Figure 1, RyR2). RyR activation is associated with major conformational changes of the P1 domain (101–103), which is hypothesized to switch the HC to the "available to open" state. A peptide dubbed RyRHCIp based on a conserved sequence on the P1 domain of the RyR was found to inhibit Cx43 HC opening in ventricular cardiomyocytes triggered by RyR2 activation with caffeine (70), while having no effect in noncardiac cells that lack the high degree of differentiation. Interestingly, modification of the second Arg in the RyRHCIp stretch of the P1 domain (Arg1027) is phenotypically associated with primary familial hypertrophic cardiomyopathy (70).

*Cx43 allocates $Na^+$ and $K^+$ channels at IDs*. At the perinexus, Cx43 HCs interact with $Na_v1.5$ (SCN5A), the pore-forming subunit of the voltage-gated $Na^+$ channel that is essential for cardiomyocyte depolarization, and Kir2.1 $K^+$ channels, associated with Andersen-Tawil syndrome and short QT syndrome (104–106). Two distinct pools of $Na_v1.5$ channels exist in the heart: one located at the ID and one at the costameres (107, 108). As a result of these Cx43–$Na^+$ channel interactions, $Na^+$ currents are larger at the ID (108) and, most importantly, reduced Cx43 expression is associated with diminished $Na_v1.5$ expression (109), thereby compromising the two main pillars of impulse conduction.

## Connexin HCs and arrhythmia

Due to the crucial role of Cx43 in the body and the heart in particular, mutants have a high risk of being eliminated at an early stage of fetal development (110–112), and thus, only a few reports link Cx43 mutations to human sudden cardiac death. Van Norstrand et al. identified two missense mutations in *GJA1* resulting in E42K and S272P mutations in Cx43 in sudden infant death syndrome (113). Additionally, Cx43 mutations have been identified as the cause of oculodentodigital dysplasia, an autosomal dominant syndrome characterized by craniofacial and limb abnormalities (114). Arrhythmias are strikingly absent in this disease except for the I130T mutant (located in the Gap19 sequence; Figure 1) that forms leaky HCs and is linked to ventricular tachycardia (17). More recently, several studies demonstrated that increased HC opening is linked to ventricular arrhythmogenesis at the cellular level, with evidence coming from mouse models of Duchenne muscular dystrophy (115–118) and of arrhythmogenic right ventricular cardiomyopathy (119), as well from human data on Cx43 HC-linked excitability disturbances leading to triggered APs (tAPs) in heart failure (77). These experimental studies will be further discussed below.

Atrial cardiomyocytes express both Cx40 and Cx43, with Cx40 showing the largest expression. Several mutations as well as a rare polymorphism have been reported in the Cx40 *GJA5* gene in human atrial fibrillation (AF) patients (120, 121), but little or nothing is known about their functional impact on Cx40-based HCs. As this Review focuses on Cx43 HCs, we include in the discussion below a recent report of Cx43 HC involvement in AF associated with a rare human mutation in the *MYL4* gene (c.234delC) as a heritable cause of AF (122).

*Duchenne muscular dystrophy*. Duchenne muscular dystrophy (DMD) is an X-linked genetic disease resulting in muscle degeneration owing to the absence of the protein dystrophin in affected males; it also leads to dystrophic cardiomyopathy, which is a major cause of patient mortality (123). In mdx mice, a genetic DMD model expressing non-functional dystrophin (further referred to as Dmd-mdx), Gonzalez et al. demonstrated that arrhythmias induced by β-adrenergic stimulation with isoproterenol, as well as the ensuing animal mortality, were significantly decreased after HC inhibition with Gap26 or Gap19 (115). ECG recordings demonstrated increased premature ventricular contractions (PVCs) in Dmd-mdx relative to wild-type animals (Figure 3A). The increased PVC frequency resulted from increased HC opening, based on ethidium bromide (EtBr) dye uptake studies. Increased HC opening resulted in depolarization of ventricular cardiomyocytes, leading to "triggered activity," i.e., above-threshold depolarization events manifested as tAPs (117), a cellular arrhythmic manifestation. Increased HC opening resulted from isoproterenol-induced nitric oxide formation, leading to nitrosylation of Cx43 at Cys271 (Figure 1) and subsequent lateralization of Cx43 (Figure 3A). Accordingly, biotinylation experiments showed an increased density of lateralized HCs (117).

In a further scrutiny of Dmd-mdx mice, Himelman et al. reported that dystrophin loss is associated with microtubule reorganization as hyperdense structures (118), which were found to enhance ROS production and oxidation of calmodulin kinase II (CaMKII) (Figure 3B). Oxidized CaMKII consequently provoked a decrease in Cx43 phosphorylation of Cx43 residues S325/S328/S330 (Figure 1) that set the stage for Cx43 remodeling, lateralization, and increased HC opening. Accordingly, the isoproterenol-triggered PVC frequency correlated well with EtBr HC dye uptake. Moreover, PVCs were absent in phosphomimetic Cx43 S325E/S328E/S330E mice, which also displayed decreased cardiomyopathy and increased survival. The QT time, reflecting the AP plateau phase and repolarization, was prolonged in Dmd-mdx mice while normal in S325E/S328E/S330E animals. The observed beneficial effect of phosphomimetic S325E/S328E/S330E is in line with the observation that phosphorylation of the Ser triplet is associated with proper localization of Cx43 to the IDs, while hypophosphorylation leads to lateralization (124–126) and increased probability of HC opening. In contrast, transgenic animals carrying a slightly different non-phosphorylatable mutant S325A/S328T/S330A showed decreased, not increased, HC activity as investigated by patch clamp approaches in mouse ventricular cardiomyocytes (127), which requires further scrutiny.

*Arrhythmogenic right ventricular cardiomyopathy*. Strict spatiotemporal control of $[Ca^{2+}]_i$ dynamics is crucial for normal cardiomyocyte function, and recent evidence demonstrated that Cx43 HC opening triggers disturbed $[Ca^{2+}]_i$ dynamics in a plakophilin-2–knockout (PKP2-KO) mouse model of arrhythmogenic right ventricular cardiomyopathy (ARVC) (119). PKP2 is a desmosomal ID protein involved in regulating intercellular junction assembly (128); it also controls gene transcription related to $Ca^{2+}$ cycling and heart rhythm (129). Mutations in *PKP2* are associated with the majority

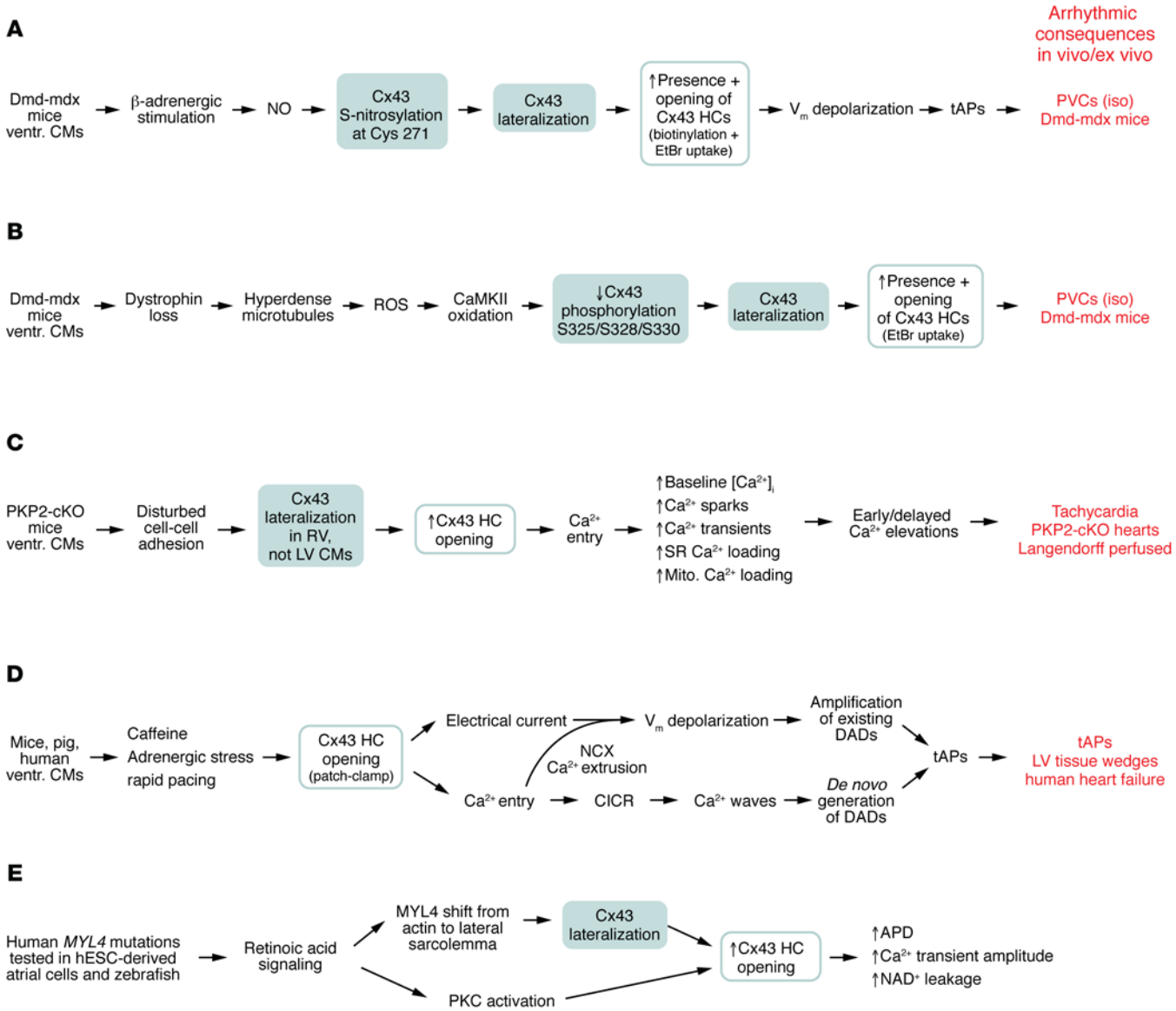


**Figure 3. Contribution of Cx43 HCs to ventricular and atrial arrhythmogenesis.** Overview of signaling cascades leading to HC-related arrhythmic responses in ventricular (**A**–**D**) and atrial cardiomyocytes (**E**). Arrhythmogenic consequences of HC opening are given for the ventricular cascades **A**–**E** and are further explained in the main text. APD, action potential duration; cKO, conditional knockout; CM, cardiomyocyte; $NAD^+$, nicotinamide adenine dinucleotide; ventr., ventricular.

of genetic causes leading to ARVC (130). Ventricular cardiomyocytes isolated from inducible-PKP2-KO (PKP2-cKO) mice before the appearance of overt cardiomyopathy (i.e., still-intact tissue) have a widened intercellular space and display Cx43 remodeling and HC lateralization in the right but not the left ventricle (119) (Figure 3C). Interestingly, the phenotype is associated with ultrastructural appearance of linear plaque-like HC arrays (119, 129, 131). At the functional level, the phenotype demonstrated abnormal $[Ca^{2+}]_i$ dynamics that were diminished in PKP2-cKO/Cx43$^{+/-}$ mice and suppressed by Gap19. The disturbed $[Ca^{2+}]_i$ dynamics entailed increased sparking frequency and $Ca^{2+}$ transient amplitudes, as well as increased sarcoplasmic reticulum (SR) and mitochondrial $Ca^{2+}$ loading, culminating in early and delayed $Ca^{2+}$ alterations as cellular arrhythmogenic signs. In addition to Gap19 inhibition of HCs, the increased $Ca^{2+}$ spark frequency was also reduced by PKC inhibitors. PKP2-cKO cardiomyocytes further displayed increased phosphorylation of RyR2 at amino acid residue T2809 located in a domain involved in modulating $Ca^{2+}$ gating. These cellular data were complemented by ECG studies in Langendorff-perfused hearts of PKP2-cKO mice, which, in contrast to wild-type animals, demonstrated long runs of ventricular tachycardia upon challenge with isoproterenol/rapid pacing (Figure 3C).

*HC-linked arrhythmogenic mechanisms in ventricular cardiomyocytes*. De Smet et al. and Lissoni et al. provided a detailed account of the mechanisms and consequences of Cx43 HC opening in response to challenge of mouse and pig left ventricular cardiomyocytes with caffeine or β-adrenergic agonists (70, 77). A typical caffeine response is represented in Figure 2E, demonstrating a slow transient inward current on which, superimposed, appear brief spike-like current events. The transient current is mediated

**Table 3. Three levels of HC contributions to arrhythmogenic responses in ventricular cardiomyocytes**

| Cause | Consequence | Reference |
|---|---|---|
| Sarcolemmal presence of permanently open HCs | Membrane depolarization leading to increased probability of DADs reaching the threshold for tAP generation | 115 |
| Spiking HC opening during $Ca^{2+}$ waves | Depolarization superimposed on existing DADs thereby increasing tAP generation | 77 |
| Burst HC opening activity directly triggering $Ca^{2+}$ waves | HC-linked microdomain $[Ca^{2+}]_i$ elevation initiating cardiomyocyte $Ca^{2+}$ waves, NCX activation, and DADs/tAPs | 77 |

by the electrogenic action of the $Na^+/Ca^{2+}$ exchange (NCX) transporter, which for every $Ca^{2+}$ extruded brings three $Na^+$ inside the cell (Figure 2G). In contrast, the spiking currents result from brief Cx43 HC opening events (first linked to Cx43 in 1990 by Pott and Mechmann, ref. 132). Other proposed channels, like sarcolemmal RyRs (133, 134), Panx1 channels (135), and the transient receptor potential channels TRPP2 (PKD2) and TRPP5 (PKD2L2) (136), were excluded (77). Atrial cardiomyocytes display similar spiking opening activity of Cx43 HCs (137). In ventricular cells, HC activity was found to vary between species, with mouse and human cardiomyocytes displaying the highest activity while activity in pig cells was lower (77). It is often assumed that the high HC opening activity in single dissociated cardiomyocytes is a by-product of cell dissociation or linked to the absence of GJs. However, macro-patch approaches mapping HC activity at cell ends showed that HC opening activity was larger in GJ-connected cardiomyocyte cell pairs than in single cardiomyocytes (77).

HC opening in ventricular cardiomyocytes at negative diastolic potential requires both caffeine stimulation and $[Ca^{2+}]_i$ elevation; importantly, $[Ca^{2+}]_i$ elevation by itself is not sufficient and neither is caffeine stimulation under conditions of strong $[Ca^{2+}]_i$ buffering (70). It was found that Cx43 interacts with RyR2, and preventing this interaction using RyRHCIp peptide blocked HC activation. These findings suggest three prerequisites to open Cx43 HCs in ventricular cardiomyocytes: (a) activation of RyR2 by caffeine, adrenergic stress, or rapid pacing; (b) $[Ca^{2+}]_i$ elevation; and (c) molecular interaction between RyR2 and Cx43 (Figure 2F).

Cx43 HC opening in ventricular cardiomyocytes can also be triggered by isoproterenol, and combined isoproterenol/rapid pacing stimulation results in very strong HC opening activity (77). These stimulation protocols are well known to increase SR $Ca^{2+}$ loading, leading to increased $Ca^{2+}$ sparking activity (138–140). However, $Ca^{2+}$ release combined with RyR2-Cx43 interaction fulfills only two, not all three, of the conditions necessary for HC activation, but it seems obvious that the third condition of RyR2 activation is mediated by $Ca^{2+}$ itself, as occurs in $Ca^{2+}$-induced $Ca^{2+}$ release (CICR).

How does HC opening lead to arrhythmogenic responses in ventricular cardiomyocytes? De Smet et al. demonstrated that HC opening frequently occurs in association with $Ca^{2+}$ waves triggered by β-adrenergic activation combined with rapid pacing (77). Such $Ca^{2+}$ waves typically lead to delayed afterdepolarizations (DADs), caused by the electrogenic consequences of NCX-mediated $Ca^{2+}$ extrusion during the wave (entry of three $Na^+$ for every $Ca^{2+}$ extruded). HC opening results in an approximately 1.6-mV depolarization per open HC and another of about 1.3 mV resulting from electrogenic effects of NCX extrusion of HC-linked elevated microdomain $[Ca^{2+}]_i$ (77) (Figure 2G and Figure 3D). As such, HC spiking activity occurring during a $Ca^{2+}$ wave may thus increase DAD amplitude and tAP frequency. This was confirmed in human ventricular cardiomyocytes from failing hearts, where HC inhibition with TAT-Gap19 significantly decreased DAD amplitude and tAP frequency.

In addition to HC activity occurring during $Ca^{2+}$ waves, HC opening was also found to precede the $Ca^{2+}$ waves. In this case, there was a brief approximately 50-millisecond delay between HC opening activity and the start of the $Ca^{2+}$ wave, suggesting a causal linkage (77). The majority of such waves started at cell ends where HC density is highest. Opening of HCs at these sites not only triggers depolarization but also leads to $Ca^{2+}$ entry and $[Ca^{2+}]_i$ elevation at HC-dyad microdomains estimated to attain 0.8 μM per HC for 1.0 mM extracellular $Ca^{2+}$ (3.4 μM for 1.8 mM external $Ca^{2+}$) (77). Such HC-initiated $Ca^{2+}$ waves invariably led to DADs and tAPs in ventricular cardiomyocytes from failing human hearts (see *De novo generation of DADs* in Figure 3D), which were effectively suppressed by TAT-Gap19. These cellular data were confirmed in arterially perfused ventricular tissue wedges from failing human hearts demonstrating significantly increased DAD rates (~1 per 3 seconds) and tAPs (~1 per 7 seconds) following 2 Hz pacing/isoproterenol, compared with wedges from non-failing hearts (Figure 3D). DAD amplitudes and DAD/tAP frequencies were all significantly reduced by TAT-Gap19 and increased by TAT-CT9.

Collectively, these observations indicate that the opening of a few Cx43 HCs per cardiomyocyte (sometimes one to four coincident HC openings; Figure 2E) may be sufficient to produce arrhythmogenic responses in ventricular cells and tissues from failing human hearts. It is important to note here that HC opening will only result in depolarization when opening occurs at negative $V_m$, i.e., during diastole. HCs are poorly selective channels with a reversal potential of around 0 mV. Consequently, HC opening at positive $V_m$, e.g., during the AP plateau or early repolarization, will result in $V_m$ changes in the direction of the 0-mV axis, i.e., opposite to the responses at negative $V_m$.

Figure 3D summarizes the signaling cascade starting from stressors (caffeine, isoproterenol, tachycardia) leading to increased HC opening in ventricular cardiomyocytes and its arrhythmic consequences in heart failure. Based on the evidence presented in the cascades of Figure 3, A–D, we conclude that arrhythmic HC contributions may occur through three distinct mechanisms summarized in Table 3 above.

*Cx43 HCs in AF*. While most evidence for arrhythmogenic contributions of HCs comes from work on ventricular cells and tissues, some evidence also points to potential arrhythmogenic involvement of HCs in the atria. Ghazizadeh et al. (141) used an original approach starting from a rare human mutation in the *MYL4* gene (Icelandic c.234delC), coding for myosin light chain-4 (MYL4) protein and representing one of the identified heritable causes of AF (122). They explored mutant *MYL4* properties in atrial cells derived

from human embryonic stem cells (hESCs) and in zebrafish\, in which the *cmlc1* gene is a putative ortholog of human *MYL4*. To include more common AF-generating mechanisms, they applied database information from atrial patient biopsies and tested specific *MYL4* mutations at the single-cell (hESC) and organ (zebrafish) levels to explore structural, functional, and transcriptional features predisposing to AF. The work pointed to involvement of retinoic acid signaling in cardiomyocyte cell polarity in mutant *MYL4* (Figure 3E) and demonstrated that MYL4 associated with F-actin in atrial biopsies from human subjects in normal sinus rhythm, while MYL4 shifted to the sarcolemma in biopsies from AF patients. MYL4 also coimmunoprecipitated with Cx43, and Cx43 association with actin was decreased in MYL4$^{-/-}$ hESCs, which we suggest removes the high $[Ca^{2+}]_i$ brake on HC activity (Figure 2D) and thus leads to increased HC opening. In terms of electrical and $Ca^{2+}$ consequences, experiments in MYL4$^{-/-}$ zebrafish demonstrated increased AP duration (APD) and $Ca^{2+}$ transient amplitudes in comparison with MYL4$^{+/+}$ animals. Interestingly, $NAD^+$, a compound known to be released through Cx43 HCs (142–144), was also elevated. These MYL4$^{-/-}$-associated alterations in APD, $Ca^{2+}$ transients, and $NAD^+$ release were all suppressed by Gap19 inhibition of Cx43 HCs. It was furthermore shown that retinoic acid signaling enhanced PKC activity and inhibition of PKC mitigated the changes in APD, $Ca^{2+}$ transients, and $NAD^+$ release. Taken together, this study brings up three reasons for increased HC function in atrial cells: (a) Cx43 lateralization, (b) PKC activation, and (c) actomyosin-linked disturbances favoring HC opening when $[Ca^{2+}]_i$ rises above 500 nM, as suggested here.

The multitude of Cx43 interactions with other proteins makes "location" of Cx43 a crucial determinant of its channel functions. In this regard, cardiomyocytes derived from induced pluripotent stem cells still lack the extreme degree of cardiomyocyte differentiation, in particular at the level of T-tubules, CICR, and the IDs where HCs reside in perinexal areas surrounding the GJ plaques (4, 58, 104–106, 145–149). Thus, conclusions regarding altered HC presence and function always need to be verified in experiments on primary cardiomyocytes.

## Conclusions

Our understanding of the factors that control Cx43 HC function and their contribution to ischemic heart disease and ventricular tachyarrhythmias is rapidly growing. Several peptide tools have become available to selectively inhibit HC opening as well as to enhance HC incorporation into GJs, which has substantially increased our comprehension of HC roles in disturbed cardiomyocyte function and basic cellular arrhythmogenic mechanisms. It must be considered, though, that despite the broad clinical use of beta blockers mitigating key molecular targets of cardiac excitability and despite clinical trials focused exclusively on GJs, none of these treatments has demonstrated a mortality benefit (45, 150, 151). As such, there is room for thinking about novel multilevel approaches aimed at preserving Cx43 trafficking, preventing HC opening and GJ closure, and driving HCs toward integration into GJ plaques that keep the syncytium connected. Thus, the stage is set to develop current insights toward novel candidate pharmacological tools for experimental as well as therapeutic application in human patients.

## Acknowledgments

Research of the LL group is supported by Research Foundation – Flanders (FWO) grants G052718N, G040720N, and G063023N. KW receives Ghent University funding for her postdoctoral fellowship and is supported by FWO grant G063023N. KRS is supported by FWO grant G0C7319N and KS/HLR by FWO grants G097021N and G063023N. LL, HLR, and GB are part of the FWO Scientific Research Network CaSign (W0.019.17N; W0.014.22N). MD received an Outstanding Investigator Award (R35-HL160840) from the National Institutes of Health (NIH) Heart, Lung, and Blood Institute.

Address correspondence to: Luc Leybaert, Physiology Group, Department of Basic and Applied Medical Sciences, Ghent University, Campus UZ Gent Block B, 3rd floor, Corneel Heymanslaan 10, B-9000 Ghent, Belgium. Phone: 32.9.3323366; Email: Luc.Leybaert@UGent.be.

1. Bukauskas FF, et al. Clustering of connexin 43-enhanced green fluorescent protein gap junction channels and functional coupling in living cells. *Proc Natl Acad Sci U S A*. 2000;97(6):2556–2561.
2. Boitano S, et al. Intercellular propagation of calcium waves mediated by inositol trisphosphate. *Science*. 1992;258(5080):292–295.
3. Veenstra RD, et al. Selectivity of connexin-specific gap junctions does not correlate with channel conductance. *Circ Res*. 1995;77(6):1156–1165.
4. Gaietta G, et al. Multicolor and electron microscopic imaging of connexin trafficking. *Science*. 2002;296(5567):503–507.
5. Beardslee MA, et al. Rapid turnover of connexin43 in the adult rat heart. *Circ Res*. 1998;83(6):629–635.
6. VanSlyke JK, et al. Conformational maturation and post-ER multisubunit assembly of gap junction proteins. *Mol Biol Cell*. 2009;20(9):2451–2463.
7. Lauf U, et al. Dynamic trafficking and delivery of connexons to the plasma membrane and accretion to gap junctions in living cells. *Proc Natl Acad Sci U S A*. 2002;99(16):10446–10451.
8. Mazet F, et al. Fate of intercellular junctions in isolated adult rat cardiac cells. *Circ Res*. 1985;56(2):195–204.
9. Severs NJ, et al. Fate of gap junctions in isolated adult mammalian cardiomyocytes. *Circ Res*. 1989;65(1):22–42.
10. Laing JG, et al. Degradation of connexin43 gap junctions involves both the proteasome and the lysosome. *Exp Cell Res*. 1997;236(2):482–492.
11. Laing JG, et al. Proteolysis of connexin43-containing gap junctions in normal and heat-stressed cardiac myocytes. *Cardiovasc Res*. 1998;38(3):711–718.
12. Rodríguez-Sinovas A, et al. Connexins in the heart: regulation, function and involvement in cardiac disease. *Int J Mol Sci*. 2021;22(9):4413.
13. Kondo RP, et al. Metabolic inhibition activates a non-selective current through connexin hemichannels in isolated ventricular myocytes. *J Mol Cell Cardiol*. 2000;32(10):1859–1872.
14. John SA, et al. Connexin-43 hemichannels opened by metabolic inhibition. *J Biol Chem*. 1999;274(1):236–240.
15. Contreras JE, et al. Metabolic inhibition induces opening of unapposed connexin 43 gap junction hemichannels and reduces gap junctional communication in cortical astrocytes in culture. *Proc Natl Acad Sci U S A*. 2002;99(1):495–500.
16. Retamal MA, et al. Cx43 hemichannels and gap junction channels in astrocytes are regulated oppositely by proinflammatory cytokines released from activated microglia. *J Neurosci*. 2007;27(50):13781–13792.
17. Dobrowolski R, et al. Some oculodentodigital dysplasia-associated Cx43 mutations cause increased hemichannel activity in addition to deficient gap junction channels. *J Membr Biol*. 2007;219(1–3):9–17.
18. Dobrowolski R, et al. The conditional connexin-43G138R mouse mutant represents a new model of hereditary oculodentodigital dysplasia in humans. *Hum Mol Genet*. 2008;17(4):539–554.
19. Wang N, et al. Selective inhibition of Cx43 hemichannels by Gap19 and its impact on myocardial

ischemia/reperfusion injury. *Basic Res Cardiol*. 2013;108(1):309.
20. Boengler K, et al. Connexin 43 in mitochondria: what do we really know about its function? *Front Physiol*. 2022;13:928934.
21. Dhein S, Salameh A. Remodeling of cardiac gap junctional cell-cell coupling. *Cells*. 2021;10(9):2422.
22. Leybaert L, et al. Connexins in cardiovascular and neurovascular health and disease: pharmacological implications. *Pharmacol Rev*. 2017;69(4):396–478.
23. Davis LM, et al. Gap junction protein phenotypes of the human heart and conduction system. *J Cardiovasc Electrophysiol*. 1995;6(10 pt 1):813–822.
24. van Kempen MJA, et al. Differential connexin distribution accommodates cardiac function in different species. *Microsc Res Tech*. 1995;31(5):420–436.
25. Vozzi C, et al. Chamber-related differences in connexin expression in the human heart. *J Mol Cell Cardiol*. 1999;31(5):991–1003.
26. Dhein S. Cardiac ischemia and uncoupling: gap junctions in ischemia and infarction. *Adv Cardiol*. 2006;42:198–212.
27. Kleber G. The potential role of Ca2+ for electrical cell-to-cell uncoupling and conduction block in myocardial tissue. *Basic Res Cardiol*. 1992;87 (suppl 2):131–143.
28. Cascio WE, et al. Ischemia-induced arrhythmia: the role of connexins, gap junctions, and attendant changes in impulse propagation. *J Electrocardiol*. 2005;38(4 suppl):55–59.
29. Solan JL, Lampe PD. Spatio-temporal regulation of connexin43 phosphorylation and gap junction dynamics. *Biochim Biophys Acta Biomembr*. 2018;1860(1):83–90.
30. Danik SB, et al. Modulation of cardiac gap junction expression and arrhythmic susceptibility. *Circ Res*. 2004;95(10):1035–1041.
31. Sánchez JA, et al. Effects of a reduction in the number of gap junction channels or in their conductance on ischemia-reperfusion arrhythmias in isolated mouse hearts. *Am J Physiol Heart Circ Physiol*. 2011;301(6):H2442–H2453.
32. Van Rijen HVM, et al. Slow conduction and enhanced anisotropy increase the propensity for ventricular tachyarrhythmias in adult mice with induced deletion of connexin43. *Circulation*. 2004;109(8):1048–1055.
33. Eckardt D, et al. Functional role of connexin43 gap junction channels in adult mouse heart assessed by inducible gene deletion. *J Mol Cell Cardiol*. 2004;36(1):101–110.
34. Tse G, Yeo JM. Conduction abnormalities and ventricular arrhythmogenesis: The roles of sodium channels and gap junctions. *Int J Cardiol Heart Vasc*. 2015;9:75–82.
35. Agullo-Pascual E, et al. Super-resolution imaging reveals that loss of the C-terminus of connexin43 limits microtubule plus-end capture and NaV1.5 localization at the intercalated disc. *Cardiovasc Res*. 2014;104(2):371–381.
36. Veeraraghavan R, et al. Mechanisms of cardiac conduction: a history of revisions. *Am J Physiol Heart Circ Physiol*. 2014;306(5):H619–H627.
37. Hoagland DT, et al. The role of the gap junction perinexus in cardiac conduction: potential as a novel anti-arrhythmic drug target. *Prog Biophys Mol Biol*. 2019;144:41–50.
38. Haugan K, et al. Rotigaptide (ZP123) improves atrial conduction slowing in chronic volume overload-induced dilated atria. *Basic Clin Pharmacol Toxicol*. 2006;99(1):71–79.
39. Hennan JK, et al. Rotigaptide (ZP123) prevents spontaneous ventricular arrhythmias and reduces infarct size during myocardial ischemia/reperfusion injury in open-chest dogs. *J Pharmacol Exp Ther*. 2006;317(1):236–243.
40. Kjølbye AL, et al. Maintenance of intercellular coupling by the antiarrhythmic peptide rotigaptide suppresses arrhythmogenic discordant alternans. *Am J Physiol Heart Circ Physiol*. 2008;294(1):H41–H49.
41. Su GY, et al. Effects of rotigaptide (ZP123) on connexin43 remodeling in canine ventricular fibrillation. *Mol Med Rep*. 2015;12(4):5746–5752.
42. Shiroshita-Takeshita A, et al. Model-dependent effects of the gap junction conduction-enhancing antiarrhythmic peptide rotigaptide (ZP123) on experimental atrial fibrillation in dogs. *Circulation*. 2007;115(3):310–318.
43. Skyschally A, et al. The antiarrhythmic dipeptide ZP1609 (danegaptide) when given at reperfusion reduces myocardial infarct size in pigs. *Naunyn Schmiedebergs Arch Pharmacol*. 2013;386(5):383–391.
44. Dhein S, et al. Improving cardiac gap junction communication as a new antiarrhythmic mechanism: the action of antiarrhythmic peptides. *Naunyn Schmiedebergs Arch Pharmacol*. 2010;381(3):221–234.
45. Engstrøm T, et al. Danegaptide for primary percutaneous coronary intervention in acute myocardial infarction patients: a phase 2 randomised clinical trial. *Heart*. 2018;104(19):1593–1599.
46. Freitas-Andrade M, et al. Danegaptide enhances astrocyte gap junctional coupling and reduces ischemic reperfusion brain injury in mice. *Biomolecules*. 2020;10(3):353.
47. Gigout S, et al. Role of gap junctions on synchronization in human neocortical networks. *Brain Res*. 2016;1637:14–21.
48. Giaume C, et al. Glial connexins and pannexins in the healthy and diseased brain. *Physiol Rev*. 2021;101(1):93–145.
49. Shintani-Ishida K, et al. Hemichannels in cardiomyocytes open transiently during ischemia and contribute to reperfusion injury following brief ischemia. *Am J Physiol Heart Circ Physiol*. 2007;293(3):H1714–H1720.
50. Hawat G, et al. Connexin 43 mimetic peptide Gap26 confers protection to intact heart against myocardial ischemia injury. *Pflugers Arch*. 2010;460(3):583–592.
51. Johansen D, et al. Ischemia induces closure of gap junctional channels and opening of hemichannels in heart-derived cells and tissue. *Cell Physiol Biochem*. 2011;28(1):103–114.
52. Hawat G, et al. Single intravenous low-dose injections of connexin 43 mimetic peptides protect ischemic heart in vivo against myocardial infarction. *J Mol Cell Cardiol*. 2012;53(4):559–566.
53. Decrock E, et al. Connexin 43 hemichannels contribute to the propagation of apoptotic cell death in a rat C6 glioma cell model. *Cell Death Differ*. 2009;16(1):151–163.
54. Falck AT, et al. The ambivalence of connexin43 Gap peptides in cardioprotection of the isolated heart against ischemic injury. *Int J Mol Sci*. 2022;23(17):10197.
55. Freitas-Andrade M, et al. Targeting MAPK phosphorylation of Connexin43 provides neuroprotection in stroke. *J Exp Med*. 2019;216(4):916–935.
56. Jiang J, et al. Interaction of α carboxyl terminus 1 peptide with the connexin 43 carboxyl terminus preserves left ventricular function after ischemia-reperfusion injury. *J Am Heart Assoc*. 2019;8(16):e012385.
57. O'Quinn MP, et al. A peptide mimetic of the connexin43 carboxyl terminus reduces gap junction remodeling and induced arrhythmia following ventricular injury. *Circ Res*. 2011;108(6):704–715.
58. Rhett JM, et al. Connexin 43 connexon to gap junction transition is regulated by zonula occludens-1. *Mol Biol Cell*. 2011;22(9):1516–1528.
59. Hunter AW, et al. Zonula occludens-1 alters connexin43 gap junction size and organization by influencing channel accretion. *Mol Biol Cell*. 2005;16(12):5686–5698.
60. Giepmans BNG, Moolenaar WH. The gap junction protein connexin43 interacts with the second PDZ domain of the zona occludens-1 protein. *Curr Biol*. 1998;8(16):931–934.
61. Bao X, et al. Mechanism of regulation of the gap junction protein connexin 43 by protein kinase C-mediated phosphorylation. *Am J Physiol Cell Physiol*. 2004;286(3):C647–C654.
62. Bao X, et al. Regulation of purified and reconstituted connexin 43 hemichannels by protein kinase C-mediated phosphorylation of Serine 368. *J Biol Chem*. 2004;279(19):20058–20066.
63. Bao X, et al. Change in permeant size selectivity by phosphorylation of connexin 43 gap-junctional hemichannels by PKC. *Proc Natl Acad Sci U S A*. 2007;104(12):4919–4924.
64. Axelsen LN, et al. Identification of ischemia-regulated phosphorylation sites in connexin43: a possible target for the antiarrhythmic peptide analogue rotigaptide (ZP123). *J Mol Cell Cardiol*. 2006;40(6):790–798.
65. Lampe PD, et al. Phosphorylation of connexin43 on serine368 by protein kinase C regulates gap junctional communication. *J Cell Biol*. 2000;149(7):1503–1512.
66. Richards TS, et al. Protein kinase C spatially and temporally regulates gap junctional communication during human wound repair via phosphorylation of connexin43 on serine368. *J Cell Biol*. 2004;167(3):555–562.
67. Vermij SH, et al. Refining the molecular organization of the cardiac intercalated disc. *Cardiovasc Res*. 2017;113(3):259–275.
68. Ponsaerts R, et al. Intramolecular loop/tail interactions are essential for connexin 43-hemichannel activity. *FASEB J*. 2010;24(11):4378–4395.
69. Iyyathurai J, et al. The SH3-binding domain of Cx43 participates in loop/tail interactions critical for Cx43-hemichannel activity. *Cell Mol Life Sci*. 2018;75(11):2059–2073.
70. Lissoni A, et al. RyR2 regulates Cx43 hemichannel intracellular Ca2+-dependent activation in cardiomyocytes. *Cardiovasc Res*. 2021;117(1):123–136.
71. De Vuyst E, et al. Ca(2+) regulation of connexin 43 hemichannels in C6 glioma and glial cells. *Cell Calcium*. 2009;46(3):176–187.
72. Zhou Y, et al. Identification of the calmodulin binding domain of connexin 43. *J Biol Chem*. 2007;282(48):35005–35017.
73. Ponsaerts R, et al. The contractile system as a

negative regulator of the connexin 43 hemichannel. *Biol Cell*. 2012;104(7):367–377.
74. D'hondt C, et al. Cx43-hemichannel function and regulation in physiology and pathophysiology: insights from the bovine corneal endothelial cell system and beyond. *Front Physiol*. 2014;5:348.
75. Wang N, et al. Connexin mimetic peptides inhibit Cx43 hemichannel opening triggered by voltage and intracellular Ca2+ elevation. *Basic Res Cardiol*. 2012;107(6):304.
76. Bol M, et al. At the cross-point of connexins, calcium, and ATP: blocking hemichannels inhibits vasoconstriction of rat small mesenteric arteries. *Cardiovasc Res*. 2017;113(2):195–206.
77. De Smet MAJ, et al. Cx43 hemichannel microdomain signaling at the intercalated disc enhances cardiac excitability. *J Clin Invest*. 2021;131(7):e137752.
78. Lopez W, et al. Mechanism of gating by calcium in connexin hemichannels. *Proc Natl Acad Sci U S A*. 2016;113(49):E7986–E7995.
79. De Vuyst E, et al. Intracellular calcium changes trigger connexin 32 hemichannel opening. *EMBO J*. 2006;25(1):34–44.
80. Iyyathurai J, et al. Peptides and peptide-derived molecules targeting the intracellular domains of Cx43: gap junctions versus hemichannels. *Neuropharmacology*. 2013;75:491–505.
81. Seki A, et al. Loss of electrical communication, but not plaque formation, after mutations in the cytoplasmic loop of connexin43. *Heart Rhythm*. 2004;1(2):227–233.
82. Bouvier D, et al. Characterization of the structure and intermolecular interactions between the connexin40 and connexin43 carboxyl-terminal and cytoplasmic loop domains. *J Biol Chem*. 2009;284(49):34257–34271.
83. Duffy HS, et al. pH-dependent intramolecular binding and structure involving Cx43 cytoplasmic domains. *J Biol Chem*. 2002;277(39):36706–36714.
84. Hirst-Jensen BJ, et al. Characterization of the pH-dependent interaction between the gap junction protein connexin43 carboxyl terminus and cytoplasmic loop domains. *J Biol Chem*. 2007;282(8):5801–5813.
85. Lissoni A, et al. Gap19, a Cx43 hemichannel inhibitor, acts as a gating modifier that decreases main state opening while increasing substate gating. *Int J Mol Sci*. 2020;21(19):7340.
86. Seki A, et al. Modifications in the biophysical properties of connexin43 channels by a peptide of the cytoplasmic loop region. *Circ Res*. 2004;95(4):e22–e28.
87. Delmar M, et al. Structural bases for the chemical regulation of Connexin43 channels. *Cardiovasc Res*. 2004;62(2):268–275.
88. Verma V, et al. Novel pharmacophores of connexin43 based on the "RXP" series of Cx43-binding peptides. *Circ Res*. 2009;105(2):176–184.
89. Gadicherla AK, et al. Mitochondrial Cx43 hemichannels contribute to mitochondrial calcium entry and cell death in the heart. *Basic Res Cardiol*. 2017;112(3):27.
90. De Bock M, et al. Connexin 43 hemichannels contribute to cytoplasmic Ca2+ oscillations by providing a bimodal Ca2+-dependent Ca2+ entry pathway. *J Biol Chem*. 2012;287(15):12250–12266.
91. Delvaeye T, et al. Blocking connexin43 hemichannels protects mice against tumour necrosis factor-induced inflammatory shock. *Sci Rep*. 2019;9(1):16623.
92. Giepmans BNG, et al. Connexin-43 interactions with ZO-1 and alpha- and beta-tubulin. *Cell Commun Adhes*. 2001;8(4–6):219–223.
93. Giepmans BNG, et al. Gap junction protein connexin-43 interacts directly with microtubules. *Curr Biol*. 2001;11(17):1364–1368.
94. Basheer WA, et al. GJA1-20k arranges actin to guide Cx43 delivery to cardiac intercalated discs. *Circ Res*. 2017;121(9):1069–1080.
95. Xiao S, et al. Auxiliary trafficking subunit GJA1-20k protects connexin-43 from degradation and limits ventricular arrhythmias. *J Clin Invest*. 2020;130(9):4858–4870.
96. Shaw RM, et al. Microtubule plus-end-tracking proteins target gap junctions directly from the cell interior to adherens junctions. *Cell*. 2007;128(3):547–560.
97. Giepmans BNG. Role of connexin43-interacting proteins at gap junctions. *Adv Cardiol*. 2006;42:41–56.
98. Li H, et al. Regulation of connexin43 function and expression by tyrosine kinase 2. *J Biol Chem*. 2016;291(30):15867–15880.
99. Saidi Brikci-Nigassa A, et al. Phosphorylation controls the interaction of the connexin43 C-terminal domain with tubulin and microtubules. *Biochemistry*. 2012;51(21):4331–4342.
100. Zheng L, et al. Calmodulin directly interacts with the Cx43 carboxyl-terminus and cytoplasmic loop containing three ODDD-linked mutants (M147T, R148Q, and T154A) that retain α-helical structure, but exhibit loss-of-function and cellular trafficking defects. *Biomolecules*. 2020;10(10):1452.
101. Serysheva II, et al. Subnanometer-resolution electron cryomicroscopy-based domain models for the cytoplasmic region of skeletal muscle RyR channel. *Proc Natl Acad Sci U S A*. 2008;105(28):9610–9615.
102. Samsó M, et al. Coordinated movement of cytoplasmic and transmembrane domains of RyR1 upon gating. *PLoS Biol*. 2009;7(4):e85.
103. Samsó M. A guide to the 3D structure of the ryanodine receptor type 1 by cryoEM. *Protein Sci*. 2017;26(1):52–68.
104. Rhett JM, et al. Cx43 associates with Na(v)1.5 in the cardiomyocyte perinexus. *J Membr Biol*. 2012;245(7):411–422.
105. Veeraraghavan R, et al. Sodium channels in the Cx43 gap junction perinexus may constitute a cardiac ephapse: an experimental and modeling study. *Pflugers Arch*. 2015;467(10):2093–2105.
106. Veeraraghavan R, et al. Potassium channels in the Cx43 gap junction perinexus modulate ephaptic coupling: an experimental and modeling study. *Pflugers Arch*. 2016;468(10):1651–1661.
107. Petitprez S, et al. SAP97 and dystrophin macromolecular complexes determine two pools of cardiac sodium channels Nav1.5 in cardiomyocytes. *Circ Res*. 2011;108(3):294–304.
108. Lin X, et al. Subcellular heterogeneity of sodium current properties in adult cardiac ventricular myocytes. *Heart Rhythm*. 2011;8(12):1923–1930.
109. Jansen JA, et al. Reduced heterogeneous expression of Cx43 results in decreased Nav1.5 expression and reduced sodium current that accounts for arrhythmia vulnerability in conditional Cx43 knockout mice. *Heart Rhythm*. 2012;9(4):600–607.
110. Nair RR, et al. Reduced expression of gap junction gene connexin 43 in recurrent early pregnancy loss patients. *Placenta*. 2011;32(8):619–621.
111. Winterhager E, Kidder GM. Gap junction connexins in female reproductive organs: implications for women's reproductive health. *Hum Reprod Update*. 2015;21(3):340–352.
112. He X, Chen Q. Reduced expressions of connexin 43 and VEGF in the first-trimester tissues from women with recurrent pregnancy loss. *Reprod Biol Endocrinol*. 2016;14(1):46.
113. Van Norstrand DW, et al. Connexin43 mutation causes heterogeneous gap junction loss and sudden infant death. *Circulation*. 2012;125(3):474–481.
114. Paznekas WA, et al. Connexin 43 (GJA1) mutations cause the pleiotropic phenotype of oculodentodigital dysplasia. *Am J Hum Genet*. 2003;72(2):408–418.
115. Gonzalez JP, et al. Selective connexin43 inhibition prevents isoproterenol-induced arrhythmias and lethality in muscular dystrophy mice. *Sci Rep*. 2015;5:13490.
116. Gonzalez JP, et al. Normalization of connexin 43 protein levels prevents cellular and functional signs of dystrophic cardiomyopathy in mice. *Neuromuscul Disord*. 2018;28(4):361–372.
117. Lillo MA, et al. S-nitrosylation of connexin43 hemichannels elicits cardiac stress-induced arrhythmias in Duchenne muscular dystrophy mice. *JCI Insight*. 2019;4(24):e130091.
118. Himelman E, et al. Prevention of connexin-43 remodeling protects against Duchenne muscular dystrophy cardiomyopathy. *J Clin Invest*. 2020;130(4):1713–1727.
119. Kim JC, et al. Disruption of $Ca^{2+}_i$ homeostasis and connexin 43 hemichannel function in the right ventricle precedes overt arrhythmogenic cardiomyopathy in plakophilin-2-deficient mice. *Circulation*. 2019;140(12):1015–1030.
120. Chaldoupi SM, et al. The role of connexin40 in atrial fibrillation. *Cardiovasc Res*. 2009;84(1):15–23.
121. Guo YH, Yang YQ. Atrial fibrillation: focus on myocardial connexins and gap junctions. *Biology (Basel)*. 2022;11(4):489.
122. Gudbjartsson DF, et al. Large-scale whole-genome sequencing of the Icelandic population. *Nat Genet*. 2015;47(5):435–444.
123. Kamdar F, Garry DJ. Dystrophin-deficient cardiomyopathy. *J Am Coll Cardiol*. 2016;67(21):2533–2546.
124. Qu J, et al. Gap junction remodeling and spironolactone-dependent reverse remodeling in the hypertrophied heart. *Circ Res*. 2009;104(3):365–371.
125. Huang RYC, et al. Identification of CaMKII phosphorylation sites in Connexin43 by high-resolution mass spectrometry. *J Proteome Res*. 2011;10(3):1098–1109.
126. Remo BF, et al. Phosphatase-resistant gap junctions inhibit pathological remodeling and prevent arrhythmias. *Circ Res*. 2011;108(12):1459–1466.
127. Hirschhäuser C, et al. Connexin 43 phosphorylation by casein kinase 1 is essential for the cardioprotection by ischemic preconditioning. *Basic Res Cardiol*. 2021;116(1):21.
128. Bass-Zubek AE, et al. Plakophilin 2: a critical scaffold for PKC alpha that regulates intercellular junction assembly. *J Cell Biol*. 2008;181(4):605–613.
129. Cerrone M, et al. Plakophilin-2 is required for transcription of genes that control calcium cycling and cardiac rhythm. *Nat Commun*. 2017;8(1):106.

130. Groeneweg JA, et al. Clinical presentation, long-term follow-up, and outcomes of 1001 arrhythmogenic right ventricular dysplasia/cardiomyopathy patients and family members. *Circ Cardiovasc Genet*. 2015;8(3):437–446.
131. van Opbergen CJM, et al. "Orphan" connexin43 in plakophilin-2 deficient hearts revealed by volume electron microscopy. *Front Cell Dev Biol*. 2022;10:843687.
132. Pott L, Mechmann S. Large-conductance ion channel measured by whole-cell voltage clamp in single cardiac cells: modulation by beta-adrenergic stimulation and inhibition by octanol. *J Membr Biol*. 1990;117(2):189–199.
133. Kondo RP, et al. Putative ryanodine receptors in the sarcolemma of ventricular myocytes. *Pflugers Arch*. 2000;440(1):125–131.
134. Zhang YA, et al. Caffeine-activated large-conductance plasma membrane cation channels in cardiac myocytes: characteristics and significance. *Am J Physiol Heart Circ Physiol*. 2007;293(4):H2448–H2461.
135. Kienitz MC, et al. Pannexin 1 constitutes the large conductance cation channel of cardiac myocytes. *J Biol Chem*. 2011;286(1):290–298.
136. Volk T, et al. A polycystin-2-like large conductance cation channel in rat left ventricular myocytes. *Cardiovasc Res*. 2003;58(1):76–88.
137. Fakuade FE, et al. Connexin hemichannels in atrial fibrillation: orphaned and irrelevant? *Cardiovasc Res*. 2021;117(1):4–6.
138. Fujiwara K, et al. Burst emergence of intracellular Ca2+ waves evokes arrhythmogenic oscillatory depolarization via the Na+-Ca2+ exchanger: simultaneous confocal recording of membrane potential and intracellular Ca2+ in the heart. *Circ Res*. 2008;103(5):509–518.
139. Song Z, et al. Stochastic initiation and termination of calcium-mediated triggered activity in cardiac myocytes. *Proc Natl Acad Sci U S A*. 2017;114(3):E270–E279.
140. Venetucci LA, et al. Increasing ryanodine receptor open probability alone does not produce arrhythmogenic calcium waves: threshold sarcoplasmic reticulum calcium content is required. *Circ Res*. 2007;100(1):105–111.
141. Ghazizadeh Z, et al. Metastable atrial state underlies the primary genetic substrate for MYL4 mutation-associated atrial fibrillation. *Circulation*. 2020;141(4):301–312.
142. Bruzzone S, et al. Connexin 43 hemi channels mediate Ca2+-regulated transmembrane NAD+ fluxes in intact cells. *FASEB J*. 2001;15(1):10–12.
143. De Flora A, et al. Autocrine and paracrine calcium signaling by the CD38/NAD+/cyclic ADP-ribose system. *Ann N Y Acad Sci*. 2004;1028:176–191.
144. Fruscione F, et al. Regulation of human mesenchymal stem cell functions by an autocrine loop involving NAD+ release and P2Y11-mediated signaling. *Stem Cells Dev*. 2011;20(7):1183–1198.
145. Parikh SS, et al. Thyroid and glucocorticoid hormones promote functional T-tubule development in human-induced pluripotent stem cell-derived cardiomyocytes. *Circ Res*. 2017;121(12):1323–1330.
146. Koivumäki JT, et al. Structural immaturity of human iPSC-derived cardiomyocytes: in silico investigation of effects on function and disease modeling. *Front Physiol*. 2018;9:80.
147. Rhett JM, Gourdie RG. The perinexus: a new feature of Cx43 gap junction organization. *Heart Rhythm*. 2012;9(4):619–623.
148. Rhett JM, et al. The perinexus: sign-post on the path to a new model of cardiac conduction? *Trends Cardiovasc Med*. 2013;23(6):222–228.
149. Veeraraghavan R, et al. The adhesion function of the sodium channel beta subunit (β1) contributes to cardiac action potential propagation. *Elife*. 2018;7:e37610.
150. Priori SG, et al. 2015 ESC Guidelines for the management of patients with ventricular arrhythmias and the prevention of sudden cardiac death: the Task Force for the Management of Patients with Ventricular Arrhythmias and the Prevention of Sudden Cardiac Death of the European Society of Cardiology (ESC). Endorsed by: Association for European Paediatric and Congenital Cardiology (AEPC). *Eur Heart J*. 2015;36(41):2793–2867.
151. Zhang XS, Xiang BR. Discontinued drugs in 2008: cardiovascular drugs. *Expert Opin Investig Drugs*. 2009;18(7):875–885.
152. Dhillon PS, et al. Relationship between connexin expression and gap-junction resistivity in human atrial myocardium. *Circ Arrhythm Electrophysiol*. 2014;7(2):321–329.
153. Kanagaratnam P, et al. Relative expression of immunolocalized connexins 40 and 43 correlates with human atrial conduction properties. *J Am Coll Cardiol*. 2002;39(1):116–123.